

Infrared Calibration Development at Fluke Corporation Hart Scientific Division

Frank Liebmann
Fluke Corporation Hart Scientific Division
799 Utah Valley Drive, American Fork, Utah 84003; 801-763-1600
frank.liebmann@hartscientific.com

ABSTRACT

A flat plate calibrator is one instrument used in calibrating IR thermometers, primarily in the 8 – 14 μm band. One such family of flat plate calibrators is the 418X Precision IR Calibrator from Fluke Corporation Hart Scientific Division. This product is calibrated with a radiometric calibration. To support this radiometric calibration and its traceability, a number of developments have been made at Hart Scientific. These developments include the construction of a new IR calibration laboratory with radiometric traceability.

This paper discusses a number of topics related to the development of IR calibration capabilities at Hart Scientific. These topics include the need for a radiometric traceability for flat plate calibrators, the traceability chain to national laboratories included in radiometric calibrations at Hart Scientific, the development of blackbody cavity baths in Hart's IR calibration laboratory, and Hart Scientific's IR uncertainty budgets.

INTRODUCTION

In the world of infrared (IR) thermometry, there has been much concern about the accuracy of IR thermometers. Contributing to this concern is a general misunderstanding of their use and operation. The two main aspects of this misunderstanding are a lack of knowledge of surface emissivity and a lack of knowledge of size of source or spot size. This is true as it applies to their use and it is also true as it applies to their calibration.

To address these two issues, Fluke - Hart Scientific has developed two new flat plate IR calibrators. These products are calibrated with a radiometric (non-contact) calibration. To properly support this calibration, Hart has developed an IR calibration laboratory with radiometrically traceable cavities as well as calibration stations for these IR calibrators.

1. 418X PRODUCTS

The 418X products are flat plate IR calibrators. The major application for these IR calibrators is the calibration of handheld IR thermometers in the 8 – 14

μm band. This range includes a bulk of the handheld IR thermometers sold today.

1.1. Why Use a Flat Plate

A near blackbody cavity is the ideal calibrator for an IR or radiation thermometer. However, due to the large spot size or size of source effect of many handheld IR thermometers, the cavity's use is impractical for calibrating devices with larger spot sizes. This necessitates the use of a flat plate for IR thermometer calibrations.

The second reason to use a flat plate is its measurement geometry. In practice most handheld IR thermometers are not used to measure the temperature of blackbodies. Instead they are used to measure surfaces having emissivity not equal to 1.0. Thus the calibration geometry of the flat plate possibly more resembles the measurement geometry of an IR thermometer in its practical use.

1.2. Use of the 8 – 14 μm Band

This paper extensively covers the use of the 8 – 14 μm band. This is because this band is common to most handheld IR thermometers. A list of handheld IR thermometers from various manufacturers is shown in Table 1. It is interesting to note that there are a number of handheld IR thermometer manufacturers that do not specify their instruments' bandwidth in their literature. They were not included in this table.

Table 1. Survey of Handheld IR Thermometers

Make and Model	Bandwidth
Craftsman 50466	6 – 14 μm
Extec 42545	6 – 14 μm
Fluke 62	6.5 – 18 μm
Fluke 66	8 – 14 μm
Fluke 572	8 – 14 μm
Metris TL400L	5 – 14 μm
Omega OSXL450	7 – 18 μm
Omega OS530	8 – 14 μm
Omega OSXL650	5 – 14 μm
Omega OSXL680	8 – 14 μm
TPI 381	7 – 14 μm
ZY Temp TN400L	5 – 14 μm
ZY Temp TN423LCE	8 – 14 μm

1.3. Description of the 418X products

The 418X products consist of 2 models, the 4180 and 4181. An illustration of the 418X is shown in Figure 1. They are flat plate calibrators with a 152 mm (6 inch) diameter surface. The two products have a combined temperature range of -15°C to 500°C . They have a number of features that make them superior to previous flat plate offerings. Among these features are their radiometric calibration and the metrology and traceability behind that calibration. Along with the radiometric calibration comes a robust uncertainty budget calculated to account for numerous factors discussed later in this paper.



Figure 1. 418X Precision IR Calibrator

1.4. Need for a Radiometric Calibration

To date, most flat plate IR calibrators rely on a contact calibration. This introduces a number of uncertainties that are difficult to account for including uncertainty in surface temperature and surface emissivity.

The first problem with relying on a contact calibration is a lack of knowledge of the surface temperature. This is due to the fact that the contact calibration does not take place on the calibrator's surface, but below it, between the calibrator and the heat source. There is a temperature difference between the contact probe and the calibrator surface. This is due to the heat flow. This problem is shown in Figure 2.

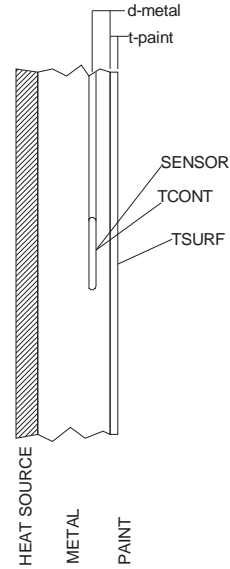


Figure 2. Surface v Sensor Temperature

One example of the effect of heat flow is the graph shown in Figure 3. This data came from an experiment conducted at Hart Scientific Division. In the experiment, a 4181 was temperature controlled at 100°C , 200°C , 300°C , 400°C and 500°C . The temperature gradient along the axial-axis of the circular plate was measured using thermocouples. Error in the thermocouple calibration was accounted for by taking a measurement using 2 thermocouples, then switching the thermocouple position. One half of the difference of these two measurements gives the temperature difference between the two points as error mathematically cancels. Temperature values were extrapolated to the calibrator's surface.

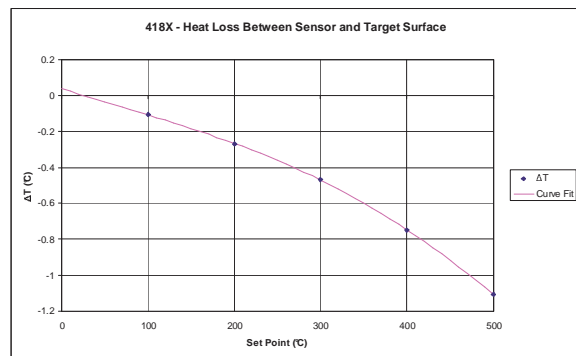


Figure 3: Heat Flow Effect at Various Temperatures

The second problem with just relying on a contact calibration is the lack of knowledge of emissivity. Emissivity is especially troublesome because it can be both wavelength and temperature dependent. This makes assuming emissivity to be an arbitrary value

questionable. Such an assumption can cause some large values in temperature uncertainties.

A surface's emissivity dependence on wavelength and temperature can be verified by Fourier Transform Infrared (FTIR) tests [1 and 2]. Results from two such tests are shown in Figure 4. These graphs show how non-gray a material can be. We define gray as a material having the same emissivity regardless of wavelength [3]. It is plain to see that a material's emissivity can vary depending on what wavelength is being measured.

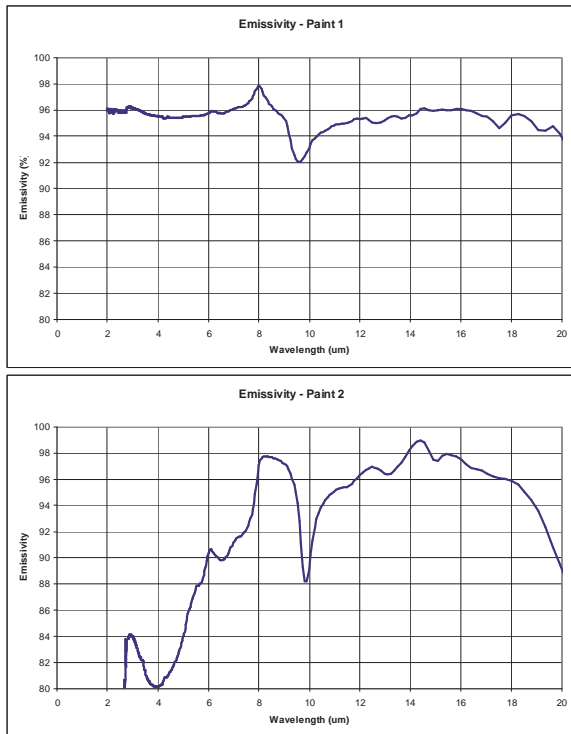


Figure 4: Results from FTIR Testing

Figure 5 shows the effect of a 1% change in average emissivity in the 8 – 14 μm band as predicted by a mathematical model (3). The temperature error caused by error in emissivity increases as the temperature gets farther from ambient.

Because of the uncertainties due to the difference between the surface temperature and the contact temperature and error due to surface emissivity, a more usable value for the display temperature can be shown to the user using a radiometric calibration. This is where the flat plate calibrator is calibrated using a highly accurate IR thermometer. The 418X radiometric calibration is described later in this paper.

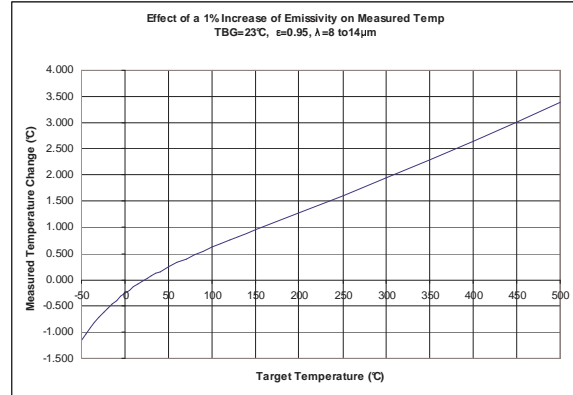


Figure 5: Effect in a 1% Change in Emissivity

2. TRACEABILITY CHAIN

The 418X calibration is done with a radiometric transfer standard, which is calibrated with Hart Scientific's cavity baths. This calibration is traceable to national labs by 2 different methods.

2.1. 418X Calibration

The display temperature on the 418X products is based on the radiometric calibration. This temperature shows the user what an IR thermometer with a given emissivity setting should read. This is called apparent temperature. The apparent temperature is defined as the temperature that an IR thermometer set to emissivity ϵ should read when pointed at the IR calibrator. In other words, the display temperature tells what temperature the calibrator appears to be to the IR thermometer.

The radiometric calibration is done with a calibrated Heitronics KT19.82II, referred to as a KT19 in this paper. This is a highly accurate IR thermometer which operates in the 8 – 14 μm band. The KT19 serves as a radiometric transfer standard. The KT19 is calibrated in cavities that will be discussed later in this paper.

The purpose for the radiometric calibration is to account for factors that cannot be accounted for with a contact calibration. As discussed earlier, the two main factors are the difference between contact temperature and surface temperature, and the difference between UUT emissivity setting and the calibrator's surface emissivity.

There are a number of steps that have been taken to lessen uncertainties in the 418X calibration.

First, the background temperature is controlled at near room temperature. Background temperature is

defined as the temperature of any object facing the surface being measured [3]. This radiation can cause the apparent temperature of a surface to change. This is especially true at lower temperatures.

Second, for both the KT19 calibration and the 418X calibration, scatter is controlled by a cooled aperture that is controlled at a constant temperature which is close to room temperature. Testing has been done to see what the effect of KT19 scatter is on measurements in Hart's cavities. This test follows a standard guideline [4] for testing size of source. Results of this are shown in Figure 6 as size of source effect data. This data was used to determine aperture diameter and calculate aperture related uncertainties.

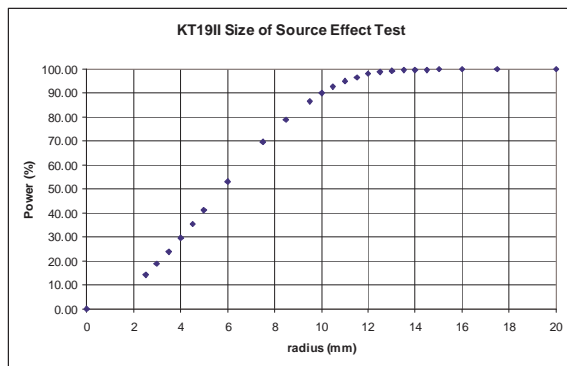


Figure 6: KT19 Size of Source Effect

Third, the lower temperature range of the 4180 is -15°C . There are 2 calibration points below ambient, -15°C and 0°C . Any radiometric calibration done between -15°C and the dew point has the risk of causing dew or ice to form on the calibrator surface. The problem with having ice or dew on the calibrator is two-fold. First, the distance between the sensor and the surface is increased by an insulating layer. This will cause the surface temperature uncertainty to increase due to lengthening the heat flow path. Second, the effect is worsened because ice or dew will also change the emissivity of the surface. Ice crystals can have an emissivity of roughly 0.98 causing apparent temperature to decrease when using the calibrator at -15°C .

Figure 7 illustrates the problem of ice build up. In this experiment, a covered 4180 calibrator was allowed to control at -15°C . The calibrator was uncovered at $T=0$ minutes. The difference between the contact temperature and the apparent temperature, measured by an IR thermometer with emissivity set to 1.000, was recorded. Initially, the apparent temperature decreases due to the higher emissivity of the ice that is forming. However, as time goes on, this temperature slowly increases due to increasing the

thickness of the insulating layer of ice.

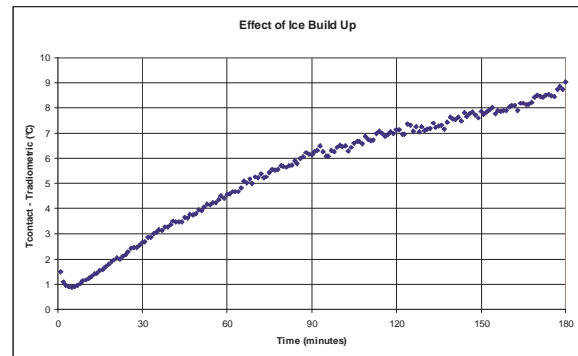


Figure 7: Radiometric Effect of Ice Build Up

To solve the problem with humidity at lower temperatures during calibration of the 4180, a purge system has been developed. This purge system involves enclosing everything between the KT19 and the 4180's surface. This area is purged with a dry gas, so that a positive pressure is maintained within this system. The dew point of the air inside the enclosure is monitored to ensure it is well below the calibration temperature.

Hart's radiometric calibration for the 418X is done with a KT19 that is calibrated with the cavity baths which are mentioned later in this paper. The 418X is set to a number of set-points. Its surface is measured by the KT19 with an emissivity setting of 0.95. This data is fed back to the 418X controller which makes the proper compensation, so that the display temperature will read within a given tolerance of the KT19's calibrated temperature. Thus the 418X has radiometric traceability.

2.2. KT19 Transfer Standard

As mentioned above, the KT19 is calibrated using Hart's cavity baths which are discussed in the next section. The KT19 calibration uses the same calibration geometry that is used in the radiometric calibration of the 418X. This means that the calibration uses the same distance from KT19 to aperture, the same aperture size and the same controlled aperture temperatures. All of these values have tolerances and are accounted for in the KT19 and 418X uncertainty budgets.

2.3. Cavity Bath Radiometric Temperature

Hart's cavity baths are described later in this paper. The KT19 is calibrated with the cavities at a number of set points. The temperature of the bath fluid during this calibration is monitored by a platinum resistance

thermometer (PRT).

2.4. TRT Calibration – Cross Check of Cavities

As mentioned earlier, the cavity bath’s fluid temperature is monitored by contact thermometry. In addition, the cavities’ radiometric temperature is cross checked with a traceable radiation thermometer (TRTII) made by Heitronics. This TRT is calibrated by the Physikalisch-Technische Bundesanstalt (PTB) in Germany. The TRT’s radiometric temperature is compared to Hart’s radiometric temperature. The difference in measurements is compared to both laboratories’ combined uncertainty. A list of the first preliminary comparison is show in Table 2. In Table 2, the 4th column lists the difference between the TRT readout temperature and the PTB cavity temperature during PTB’s calibration. The 5th column lists the difference between the TRT readout temperature and the Hart’s cavity temperature during Hart’s calibration. The 6th column lists the difference in radiometric temperatures between the two laboratories. The 7th and 8th column lists the uncertainties from PTB and Hart respectively.

Table 2: Initial TRT Cross Check Results

Temperature	Spectral Band	Hart Bath	$T_{TRT}-T_{CAV}$ at PTB (°C)	$T_{TRT}-T_{CAV}$ at Hart (°C)	$T_{HART}-T_{PTB}$ (°C)	U_{PTB} (°C)	U_{HART} (°C)
30° C	8-14 μm	LT	0.29	0.337	0.046	0.04	0.07
100 °C	8-14 μm	LT	0.75	0.644	-0.106	0.11	0.1
100 °C	8-14 μm	MT	0.75	0.660	-0.089	0.11	0.1
200 °C	8-14 μm	MT	0.8	0.568	-0.232	0.3	0.16
200 °C	8-14 μm	HT	0.8	0.649	-0.151	0.3	0.16
300 °C	3.9 μm	HT	0.8	0.997	0.197	0.2	0.20
420 °C	3.9 μm	HT	0.33	0.281	-0.048	0.1	0.17

2.5. Comparison of Cavities’ Radiometric Temperature

There are a limited number of points within Hart’s cavity bath temperature range that are covered by more than one bath. At those points, radiometric temperature has been compared. A summary of one such comparison done with a TRT is listed in Table 3. Columns 2 to 4 list the difference between TRT readout temperature and contact temperature. The 5th column lists the difference in radiometric temperature between the two cavities. The 6th column lists Hart’s radiometric uncertainty for the cavity.

Table 3: Comparison of Radiometric Temperatures

Temperature	$T_{TRT}-T_{CAV}$ LT Bath (°C)	$T_{TRT}-T_{CAV}$ MT Bath (°C)	$T_{TRT}-T_{CAV}$ HT Bath (°C)	Temperature Difference (°C)	U_{HART} (°C)
100 °C	0.6435	0.6608	NA	0.0173	0.10
200 °C	NA	0.5675	0.6489	0.0814	0.16

3. DEVELOPMENT OF CAVITY BATHS

3.1. IR Calibration Facilities at HS

To facilitate radiometric calibrations, Hart Scientific has developed 3 cavity baths for use in Hart’s new Infrared Calibration Laboratory. These baths are summarized in Table 4. They are based on existing Hart baths and use a cylinder-cone cavity that is 304 mm (12 inches) deep and 51 mm (2 inches) in diameter with an conical angle of 120°. These baths are shown in Figure 8. The cavities have emissivity greater than 0.999. This number was verified by modeling with STEEP3 [5, 6, and 7] which is discussed later in this paper.

Table 4: Details of IR Cavity Baths

Cavity Bath	Temperature Range	Built with Hart Model Number
Low Temperature (LT)	-25°C to 100°C	7038
Middle Temperature (MT)	100°C to 250°C	7024
High Temperature (HT)	200°C to 500°C	7050



Figure 8: Cavity Baths in Calibration Lab

Hart’s cavity bath fluid temperature is monitored by Hart Scientific Model 5626 PRTs that are calibrated in Hart’s Primary Calibration Laboratory. Their

calibration is traceable to NIST. The cavity's radiometric temperature is cross-checked by a Heitronics TRTII [8] that is calibrated by PTB in Germany [9]. The TRTII was a result of Euromet's Traceability in Infrared Radiation Thermometry (TRIRAT) Project [10]. An illustration of this traceability is shown in Figure 9.

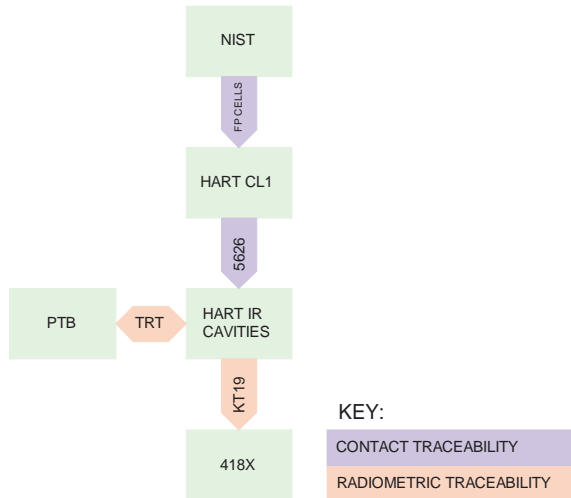


Figure 9: 418X Traceability

To gain better temperature uniformity on the cavity walls, the end of the cavity is purged with dried shop air that is heated to the bath temperature by a heat exchanger in the bath fluid.

3.2. STEEP3 Modeling

Hart has done experimentation to measure the temperature on the cavity walls by contact thermometry. Results from these tests are shown in Figure 10. These results are fed back to the STEEP 3 model. This model revealed the results in Table 5. This table shows the effective emissivities at various temperatures plus the isothermal emissivity.

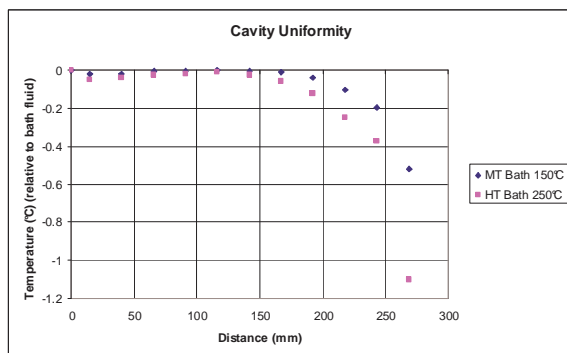


Figure 10: Temperature Uniformity of Cavity Walls

Table 5: STEEP 3 Modeling Results of Hart's Cavities

Bath	Bath Temperature	Effective Emissivity
LT & MT	Isothermal	0.9996
LT	-15°C	0.9998
LT	0°C	0.9997
LT	50°C	0.9995
LT & MT	100°C	0.9994
MT	150°C	0.9994
MT	200°C	0.9993
MT	250°C	0.9993
HT	Isothermal	0.9996
HT	200°C	0.9993
HT	250°C	0.9992
HT	300°C	0.9992
HT	350°C	0.9992
HT	400°C	0.9992
HT	450°C	0.9992
HT	500°C	0.9991

To verify Hart's cavity modeling technique, STEEP3 was used to model cavities in a number of published papers. The results of this modeling are shown in Table 6.

Table 6: Examples of STEEP3 Modeling Comparison

Cavity	Shape	Emissivity	
		From Paper	From STEEP3
Fowler[11]	Cone	0.9997±0.0003	0.9998
Ishii, Kobayashi and Sakuma[12]	Cylinder-cone	0.973 – 0.998	0.974 – 0.999
Sakuma and Ma [13]	Cylinder-cone	0.999	0.999
Sakuma and Ma [13]	Cylinder	0.999	0.999
Ma[14]	Cylinder (D=2.0mm)	0.9999	1.0000
Ma[14]	Cylinder (D=6.9mm)	0.9996	0.9997
Ma[14]	Cylinder (D=12.7mm)	0.9989	0.9990

4. HART'S IR UNCERTAINTY BUDGETS

Hart's IR uncertainty budgets are the result of much research into the uncertainties related to IR thermometry. The determination and calculation of these uncertainties involves a complex process of calculation and experimentation.

4.1. Determination of Uncertainties

The determination of Hart's uncertainties is a complex process. Where possible, experimentation has been performed to provide the uncertainty budgets with type 'A' uncertainties. Where experimentation is not possible, modeling has been

performed to provide knowledge of the uncertainty. Two examples of this are the determination of cavity effects and determination of the effects of aperture temperature. Cavity effects are the effects of the cavity not acting as a perfect blackbody. These effects are evaluated in STEEP 3 making them a type 'B' uncertainty. The effects of aperture temperature were evaluated by experimentation. The aperture temperature was varied, and the change in radiometric temperature was noted at several temperatures. The knowledge of the change in radiometric temperature versus the change in aperture temperature was used to calculate the effect of aperture temperature uncertainty in the KT19 uncertainty budget.

4.2. Evaluation of Uncertainties

As suggested by uncertainty budget guidelines [15], uncertainties are evaluated using the system's measurement equation. This measurement equation is shown in (3). Note that S is the signal detected by the IR thermometer. In this equation, signal received during calibration is compared to signal received during use (designated by S_{CAL} and S_{MEAS} in both (3) and (4)). This is what an IR thermometer does internally. The signal received by the IR thermometer

consists of the signal emitted by the object being measured (S_{MEAS}) plus the signal reflected from the background (S_{BG}) plus the signal from the aperture (S_{APE}). The signal from the calibrator is attenuated by the aperture ($1-\beta$). In addition, the signal is attenuated by the combined effects of atmosphere and the IR thermometer's measurement system (α). In all cases the emissivity of objects is considered (ϵ). Thus the IR measurement system is modeled.

This general equation is evaluated using a Planckian model. This model evaluates the measurement equation over the IR thermometer's spectral response and considers the calibrator's emissivity, aperture geometry and background temperature. This equation is difficult to solve. It must be solved using an iterative method. The integral must be evaluated numerically. However, it does accurately model various aspects of the system making it a complete model for the system. The measurement equation in Planckian form is shown in (4). References to the variables used are shown in Table 7. Previous publication has suggested the Sakuma-Hattori Equation or a narrow band form of the Planck Equation should be used [16]. In the case of the 418X, these were not used because of the wide band effects of emissivity and spectral response.

$$\begin{aligned}
 S_{CAL} &= \beta_{CAL} \alpha_{CAL} [\epsilon_{CAL} S_{CAV} + (1 - \epsilon_{CAL}) S_{BG-CAL}] + (1 - \beta_{CAL}) \alpha_{CAL} S_{APE-CAL} \\
 S_{MEAS} &= \beta_{MEAS} \alpha_{MEAS} [\epsilon_{TGT} S_{TGT} + (1 - \epsilon_{TGT}) S_{BG-MEAS}] + (1 - \beta_{MEAS}) \alpha_{MEAS} S_{APE-MEAS} \\
 S_{CAL} &= S_{MEAS}
 \end{aligned} \tag{3}$$

$$\begin{aligned}
 S_{CAL} &= \pi_{1L} \left[\beta \int_0^{\infty} \frac{\alpha_{CAL}(\lambda) \epsilon_{CAV}(\lambda)}{\lambda^5 \left[\exp\left(\frac{c_2}{\lambda T_{CAL}}\right) - 1 \right]} d\lambda + \int_0^{\infty} \frac{\alpha_{CAL}(\lambda) [1 - \epsilon_{CAV}(\lambda)]}{\lambda^5 \left[\exp\left(\frac{c_2}{\lambda T_{BG-CAL}}\right) - 1 \right]} d\lambda \right] + (1 - \beta) \int_0^{\infty} \frac{\alpha_{CAL}(\lambda)}{\lambda^5 \left[\exp\left(\frac{c_2}{\lambda T_{APE-CAL}}\right) - 1 \right]} d\lambda \\
 S_{MEAS} &= \pi_{1L} \left[\beta \int_0^{\infty} \frac{\alpha_{MEAS}(\lambda) \epsilon_{TGT}(\lambda)}{\lambda^5 \left[\exp\left(\frac{c_2}{\lambda T_{TGT}}\right) - 1 \right]} d\lambda + \int_0^{\infty} \frac{\alpha_{MEAS}(\lambda) [1 - \epsilon_{TGT}(\lambda)]}{\lambda^5 \left[\exp\left(\frac{c_2}{\lambda T_{BG-MEAS}}\right) - 1 \right]} d\lambda \right] + (1 - \beta) \int_0^{\infty} \frac{\alpha_{MEAS}(\lambda)}{\lambda^5 \left[\exp\left(\frac{c_2}{\lambda T_{APE-MEAS}}\right) - 1 \right]} d\lambda \\
 S_{CAL} &= S_{MEAS}
 \end{aligned} \tag{4}$$

4.3. KT19 and 418X Uncertainty Budgets

The KT19 uncertainty budget is shown in Appendix 1. The 4180 and 4181 uncertainty budgets are shown in Appendix 2. The parts of the measurement equation used to calculate the effect of each uncertainty is shown in Table 7. The third column

refers to which uncertainties are being accounted for by each symbol.

Table 7: Measurement Equation and Fluke Hart Scientific’s Uncertainty Budget

Symbol	Description	Uncertainty Budget
β_{CAL}	Transmission through aperture – Calibration	u_{12}
$\alpha_{CAL}(\lambda)$	System Transmission – Calibration	u_{11}
$\epsilon_{CAL}(\lambda)$	Cavity Emissivity	u_{14}
T_{CAV}	Cavity Temperature	$u_1 - u_{10}$
T_{BG-CAL}	Background Temperature – Calibration	u_{14}
$T_{APE-CAL}$	Aperture Temperature – Calibration	u_{13}
β_{MEAS}	Transmission through aperture – Measurement	u_{r9}
$\alpha_{MEAS}(\lambda)$	System Transmission – Calibration	$u_{r5} - u_{r7}$
$\epsilon_{TGT}(\lambda)$	Target Emissivity	u_{r5}
T_{TGT}	Target Temperature	$u_{r1} - u_{r4}, u_{r6}, u_{r10}, u_{r12} - u_{r18}$
$T_{BG-MEAS}$	Background Temperature – Measurement	u_{r11}
$T_{APE-MEAS}$	Aperture Temperature – Measurement	u_{r8}

CONCLUSION

The 418X project has resulted in a new measurement capability for Fluke Corporation Hart Scientific Division. A radiometric calibration has been established as the standard calibration for these units.

As a result an infrastructure to support this calibration has been developed. This infrastructure includes radiometric transfer standards and blackbody cavities to support the 418X calibration. These developments plus education of the user will help to bring more accuracy and metrology to lower temperature IR thermometry.

ACKNOWLEDGEMENTS

The author greatly appreciates the help of many people in developing this technique in calculating IR thermometry uncertainties. Among the people who have helped are Tom Wiandt, Mike Hirst and Rick Walker of Fluke Corporation Hart Scientific Division; Ingrid Gooding of Fluke; Patrick Parker, Alex Nikittin, Steve King, Medwin Schreher, Thomas Heinke and Reno Gärtner of Raytek; Leonard Hanssen, Benjamin Tsai, Sergey Mekhontsev and Howard Yoon of NIST and Kendall Johnson of the Space Dynamics Laboratory at Utah State University.

REFERENCES

1. L.M. Hanssen, A.V. Prokhorov, V.B.

Khromchenko and S.N. Mekhontsev, “Comparison of Direct and Indirect Methods of Spectral Infrared Emittance Measurement”, Proceedings of TEMPMEKO 2004, pp. 539-544, 2004.

2. “L.M. Hanssen, V.B. Khromchenko and S.N. Mekhontsev, Infrared Spectral Emissivity Characterization Facility at NIST”, Proceedings of SPIE, 5405, pp. 1-12, 2004.

3. D.P. DeWitt G.D. Nutter, Theory and Practice of Radiation Thermometry, Wiley Interscience, New York, 1988, pp. 41-43, 72-73, 194.

4. 1256 - 95 in Annual Book of ASTM Standards Vol. 14.03, ASTM International, West Conshohocken, PA, 2005, pp. 490-491.

5. A.V. Prokhorov and L.M. Hanssen, “Effective Emissivity of a Cylindrical Cavity with an Inclined Bottom”, Metrologia, Vol. 41, pp. 421-431, 2004.

6. V.I. Sapritsky and A.V. Prokhorov, “Spectral Effective Emissivities of Nonisothermal Cavities Calculated by the Monte Carlo Method”, Applied Optics, Vol. 34, No. 25, pp. 5645-5652, 1995.

7. A.V. Prokhorov, “Monte Carlo Method in Optical Radiometry”, Metrologia, Vol. 35, pp. 465-471, 1998.

8. O. Struß, “Transfer Radiation Thermometer Covering the Temperature Range from -50°C to 1000°C”, AIP Conference Proceedings, Vol. 684, pp. 565-570, 2003.

9. J. Hollandt, R. Friedrich, B. Gutschwager, D.R. Taubert, J. Hartmann, “High-accuracy Radiation Thermometry at the National Metrology Institute of Germany, the PTB”, High Temperatures - High Pressures, Vol. 35/36, pp. 379-415, 2003/2004.

10. E. van der Ham, Traceability in Infrared Radiation Thermometry -50°C to 800°C Final Report on the TRIRAT Project, 2001.

11. J.B. Fowler, “A Third Generation Water Bath Based Blackbody Source”, Journal of Research of the National Institute of Standards and Technology, Vol. 100, Num. 5, pp. 591-599, 1995.

12. J. Ishii, M. Kobayashi, and F. Sakuma, "Effective Emissivities of Black-body Cavities with Grooved Cylinders", *Metrologia*, Vol. 35, pp. 175-180, 1998.
13. F. Sakamura and L. Ma, "Cavity Emissivity of Fixed-Point Blackbody", *SICE 2003 Annual Conference*, Vol. 2, pp. 2187-2190, 2003.
14. C.K. Ma, "Method for the Measurement of the Effective Emissivity of a Cavity", *Proceedings of TEMPMEKO 2004*, pp. 575-580, 2004.
15. U. S. Guide to the Expression of Uncertainty in Measurement, John A. Wehrmeyer, Chair (National Conference of Standards Laboratories, Boulder, CO, 1997), pp. 4-8.
16. F. Sakuma, M. Kobayashi, "Interpolation Equations of Scales of Radiation Thermometers", *Proceedings of TEMPMEKO '96*, pp. 305-310.

APPENDIX 1: KT19 UNCERTAINTIES

Uncertainties	Denot.	Type	Dist	Uncertainty (°C)				
				-15	50	100	350	500
Bath Temperature Measurement								
PRT calibration and characterization	u1	A	rect	0.0120	0.0120	0.0120	0.0180	0.0280
PRT stability (long term)	u2	A	rect	0.0100	0.0120	0.0140	0.0240	0.0290
Measurement noise	u3	A	norm	0.0015	0.0019	0.0022	0.0034	0.0038
PRT self-heating	u4	B	norm	0.0015	0.0015	0.0015	0.0015	0.0015
PRT stem effect	u5	B	rect	0.0020	0.0020	0.0020	0.0020	0.0020
Readout accuracy	u6	B	rect	0.0014	0.0018	0.0022	0.0039	0.0050
KT19 Radiation measurement								
RT readout resolution	u7	A	rect	0.0031	0.0016	0.0011	0.0005	0.0005
RT ambient temperature	u8	A	norm	0.0100	0.0100	0.0100	0.0100	0.0100
RT noise	u9	A	rect	0.0400	0.0250	0.0200	0.0250	0.0350
RT repeatability	u10	B	norm	TBD	TBD	TBD	TBD	TBD
Atmospheric losses	u11	B	norm	0.0050	0.0068	0.0083	0.0187	0.0263
Aperture losses	u12	B	norm	0.0047	0.0070	0.0091	0.0224	0.0322
Aperture temperature	u13	A	rect	0.0078	0.0040	0.0028	0.0022	0.0046
Cavity effects	u14	B	rect	0.1000	0.1000	0.1000	0.1900	0.3100
Combined standard uncertainty	uc	k=1	normal	0.063	0.061	0.060	0.113	0.183
Combined expanded uncertainty (k=2)	U	k=2	normal	0.127	0.122	0.121	0.226	0.366

APPENDIX 2: PRELIMINARY 418X RADIOMETRIC UNCERTAINTIES

4180 Uncertainties	Denot.	Type	Dist	Factor	Uncertainty (°C)				
					-15	0	50	100	120
Reference radiometer related uncertainties									
RT calibration	ur1	A	norm	2.00	0.1267	0.1242	0.1216	0.1208	0.1211
RT stability (long term)	ur2	A	rect	1.73	0.1000	0.0700	0.0700	0.1000	0.1000
RT noise	ur3	A	rect	1.73	0.0590	0.0350	0.0390	0.0470	0.0520
RT readout resolution	ur4	A	rect	1.73	0.0031	0.0026	0.0016	0.0011	0.0010
RT spectral response and target emissivity	ur5	B	norm	2.00	0.0681	0.0366	0.0327	0.0802	0.0972
RT ambient temperature	ur6	A	norm	2.00	0.0100	0.0100	0.0100	0.0100	0.0100
Atmospheric losses	ur7	B	norm	2.00	0.0050	0.0054	0.0068	0.0083	0.0090
Aperture temperature	ur8	B	norm	2.00	0.0078	0.0064	0.0040	0.0025	0.0019
Aperture losses	ur9	A	norm	2.00	0.0047	0.0052	0.0070	0.0091	0.0099
Repeatability	ur10	A	norm	2.00	TBD	TBD	TBD	TBD	TBD
Background temperature	ur11	B	rect	1.73	0.0074	0.0063	0.0040	0.0029	0.0027
Control related uncertainties									
Display resolution	ur12	B	rect	1.73	0.0050	0.0050	0.0050	0.0050	0.0050
Hysteresis	ur13	A	rect	1.73	0.0000	0.0010	0.0020	0.0010	0.0000
Repeatability	ur14	A	norm	2.00	0.0050	0.0020	0.0020	0.0040	0.0040
Temperature settling	ur15	A	rect	1.73	0.0100	0.0100	0.0100	0.0100	0.0100
Target temperature related uncertainties									
Uniformity	ur16	B	rect	1.73	0.0120	0.0120	0.0120	0.0200	0.0250
Z-axis temperature loss	ur17	B	norm	2.00	0.0096	0.0056	0.0068	0.0195	0.0244
Radiometric curve fit	ur18	B	rect	1.73	0.0100	0.0100	0.0150	0.0300	0.0300
Combined standard uncertainty	uc	k=1	normal		0.099	0.080	0.080	0.100	0.105
Combined expanded uncertainty (k=2)	U	k=2	normal		0.199	0.160	0.159	0.200	0.210

4181 Uncertainties	Denot.	Type	Dist	Factor	Uncertainty (°C)				
					35	100	250	350	500
Reference radiometer related uncertainties									
RT calibration	ur1	A	norm	2.00	0.1231	0.1208	0.1223	0.1463	0.2262
RT stability (long term)	ur2	A	rect	1.73	0.0700	0.1000	0.1000	0.1100	0.1200
RT noise	ur3	A	rect	1.73	0.0380	0.0550	0.0850	0.1050	0.1400
RT readout resolution	ur4	A	rect	1.73	0.0018	0.0011	0.0007	0.0006	0.0005
RT spectral response and target emissivity	ur5	B	norm	2.00	0.0154	0.0802	0.1623	0.2038	0.2917
RT ambient temperature	ur6	A	norm	2.00	0.0100	0.0100	0.0100	0.0100	0.0100
Atmospheric losses	ur7	B	norm	2.00	0.0063	0.0083	0.0120	0.0141	0.0187
Aperture temperature	ur8	B	norm	2.00	0.0045	0.0028	0.0019	0.0020	0.0022
Aperture losses	ur9	A	norm	2.00	0.0064	0.0091	0.0138	0.0165	0.0224
Repeatability	ur10	A	norm	2.00	TBD	TBD	TBD	TBD	TBD
Background temperature	ur11	B	rect	1.73	0.0045	0.0029	0.0020	0.0018	0.0015
Control related uncertainties									
Display resolution	ur12	B	rect	1.73	0.0050	0.0050	0.0050	0.0050	0.0050
Hysteresis	ur13	A	rect	1.73	0.0000	0.0050	0.0050	0.0050	0.0050
Repeatability	ur14	A	norm	2.00	0.0020	0.0040	0.0070	0.0090	0.0120
Temperature settling	ur15	A	rect	1.73	0.0100	0.0100	0.0100	0.0100	0.0100
Target temperature related uncertainties									
Uniformity	ur16	B	rect	1.73	0.0120	0.0180	0.0280	0.0320	0.0420
Z-axis temperature loss	ur17	B	norm	2.00	0.0032	0.0192	0.0444	0.0572	0.0824
Radiometric curve fit	ur18	B	rect	1.73	0.0250	0.0500	0.0500	0.0500	0.0600
Combined standard uncertainty	uc	k=1	normal		0.079	0.104	0.134	0.160	0.222
Combined expanded uncertainty (k=2)	U	k=2	normal		0.159	0.207	0.267	0.320	0.444